IEEE Access
Multidisciplinary | Rapid Review | Open Access Journal

Received January 27, 2020, accepted February 9, 2020, date of publication February 18, 2020, date of current version February 27, 2020.

Digital Object Identifier 10.1109/ACCESS.2020.2974658

Research on the Steam Valve Joystick Loading System and Its Control Strategy

BING ZHANG[1], HUA HUANG[1], JIAMIN CAI[1], ZILIANG JIANG[1], AND PENGFEI QIAN[1,2]
[1]School of Mechanical Engineering, Jiangsu University, Zhenjiang 212013, China
[2]State Key Laboratory of Fluid Power and Mechatronic Systems, Zhejiang University, Hangzhou 310027, China

Corresponding authors: Bing Zhang (zhangbing@ujs.edu.cn) and Pengfei Qian (pengfeiqian@ujs.edu.cn)

This work was supported in part by the National Natural Science Foundation of China under Grant 51805215 and Grant 51605194, in part by the Starting Foundation of Jiangsu University Advanced Talent under Grant 14JDG048, in part by the Open Foundation of the State Key Laboratory of Fluid Power and Mechatronic Systems under Grant GZKF-201819, and in part by the Youth Talent Development Program of Jiangsu University.

ABSTRACT In this paper, an idea about the hydraulic loading device is proposed to simulate the working mechanical environment of the steam valve joystick. The simulation based on the mathematical model of active and passive loading system is utilized to reveal that the stiffness of connection components in loading system has an important influence on the control accuracy of the system. Additionally, the paper provides a design on the structure of the connecting components of valve stem. For the control strategy, a dual inertia link is used to stabilize the system. Besides, a compensation method of partial structural invariance is adopted to reduce the influence of redundant force in passive loading test. Finally, The development mode of control engineering based on xPC rapid control prototype model is used to validate the loading system. The simulation and experimental results show that the dual inertia link and compensation method are effective techniques, and the passive loading error can be controlled within the tolerance of 300N.

INDEX TERMS Hydraulic loading system, dual inertia link stabilization, principle of partial structure invariance, xPC rapid control prototype.

I. INTRODUCTION

Steam valves of steam turbines are important components in the regulation and protection system of steam turbines, which play a key role in the safe operation of steam turbines [1]. The opening and closing of the valve is controlled by the stem of the steam valve which moves in a straight line under the action of the cam linkage mechanism to drive the steam valve to achieve different openings. When the steam valve moves at different steam valve openings, the force acting on the stem is also different. In order to verify the reliability of the designed stem, a loading system is needed to simulate the actual working mechanical environment of the stem [2]. The main factor affecting the control accuracy of the hydraulic loading system is redundant force, which is generated by the additional flow caused by the passive movement of the loading system. Xiaohong Jin et al. studied the hydraulic redundant force to obtain the redundant force expression in frequency domain, and pointed out that the main factor affecting the redundant force was the velocity disturbance of the loaded object [3]. Mengwen Zhao et al. utilized the phase-plane feedforward method to restrain the redundant force in the high frequency band of the aircraft steering gear loading system, which improved the fault-tolerant performance of the system in the high frequency band and the tracking ac curacy of the high frequency load spectrum [4]. Based on the analysis of the mechanism of redundant moment in electro-hydraulic load simulator, Geqiang Li proposed a synchronous structure decoupling method, and designed double-layer compound actuator, which fundamentally solved the problem of redundant moment, but only limited to moment loading [5]. Jingfu Wang et al. adopted parallel control with two valves to improve the restraint performance of the loading system on redundant force, but increased the hardware cost of the force loading system [6]. Panguo Qi and others conducted in-depth research on the force sensing simulation in the maneuvering loading system, which compensated the load inertia. Also, a robust controller based on the μ synthesis theory was designed to enhance the robustness of the force sensing simulation system. However, the real-time application of the robust controller has not been verified [7]–[9]. A nonlinear disturbance observer (NDO) was used by

The associate editor coordinating the review of this manuscript and approving it for publication was Zhuang Xu.

M. Khamar to reduce the influence of the uncertainties and external disturbance in the control method of the knee [10]. In order to improve the wire rope tension coordination control performance of the double-rope winding hoisting system, a robust nonlinear adaptive back-stepping controller combined with a NDO was proposed by Zhu *et al.* [11]. Two output feedback controllers were proposed by Guichao Yang et al. for motion control of double-rod electro-hydraulic servo actuators with matched and mismatched disturbances rejection. All of them employed a linear extended state observer to achieve real-time estimates of the unmeasured system states. The matched disturbance, and a NDO were introduced to estimate the largely unknown mismatched disturbance at the same time [12]. A state-space representation of model predictive control model predictive controller (MPC) was proposed by Haibo Yuan to accurate force tracking of an electro-hydraulic servo system [13]. Weiwei Gu proposed an output feedback with the integration of an extended state observer (ESO) to improve the ability of the traditional MPC to redundant disturbances evidently [14]. Through experiments and simulations, Wei Han verified that brake-by-brake control system achieves satisfactory tracking performance and robustness in the presence of uncertainty, nonlinearity and disturbance [15]. Xiuxing Yin et al. proposed a control strategy combining pitch angle controller with adaptive control, which has a good performance for accurate pitch angle tracking and generator power control, regardless of various uncertainties and interference [16]. Yong Sang et al. studied the bidirectional synchronous control of electro-hydraulic servo loading system. The mechanism of the coupling between two cylinders from two directions was discussed. Simultaneously, a bidirectional synchronous iterative learning control method was designed to improve the tracking performance, robustness and compensate synchronization errors [17]. Kai Guo proposed a nonlinear cascade controller based on an extended disturbance observer to track desired position trajectory for electro-hydraulic single-rod actuators in the presence of both external disturbances and parameter uncertainties [18]. In order to diminish the dynamic disturbances in some multi-degree-of-freedom manipulators driven by electro-hydraulic actuators, Qing Guo proposed a state feedback control of the cascade electro-hydraulic system based on a coupled disturbance observer with back-stepping [19]. A novel dynamic surface disturbance rejection control with synchronous compensation is proposed by Chenghu Jing to improve the torque tracking performance of electro-hydraulic load simulator [20]. In order to improve the dynamic response and disturbance rejection of an electrical-mechanical-actuator (EMA) and simplify control parameters tuning, a robust high-dynamic servo system based on linear active disturbance rejection control was proposed by Chunqiang Liu for an EMA employing a permanent magnet synchronous motor [21]. A feedforward force controller including modified force inverse model compensator and velocity feedforward compensator was combined by Gang Shen with an internal model control to compensate the redundant force disturbance caused by active motion of shaking table and to obtain high fidelity force loading tracking performance [22]. Cheng-wen Wang et al. put forward a kind of a control method which considered not only the actuator motion disturbance, but also considered the nonlinear characteristic of the loading system and parameter uncertainty of high-performance [23]. The control strategy of rapid control prototype based on xPC can use graphical programming language to carry out the control strategy of researchers quickly, and release the researchers from complicated programming work, which enable them to focus on the algorithm design. Therefore, the control strategy has important engineering value and is widely used.

In this paper, active and passive loading of steam valve stem is realized according to the requirement of mechanical environment simulation of steam valve stem. The electro-hydraulic loading system is stabilized by double inertia links, and the redundant force of the loading system is restrained by the principle of structural invariance. The reasonable range of stiffness of the stem connecting assembly for the loading system is obtained through the simulation research, and then the connecting assembly is designed with its stiffness analyzed. Finally, the real-time control system of loading system is developed based on xPC rapid control prototype method and experimental research is carried out.

II. MODELING OF STEAM STEM LOADING SYSTEM

The steam stem force loading system designed in this paper can be used to load five steam stem at the same time, and each channel can be controlled independently or five channels can be loaded simultaneously. The single channel configuration of the loading system is shown in Fig. 1.

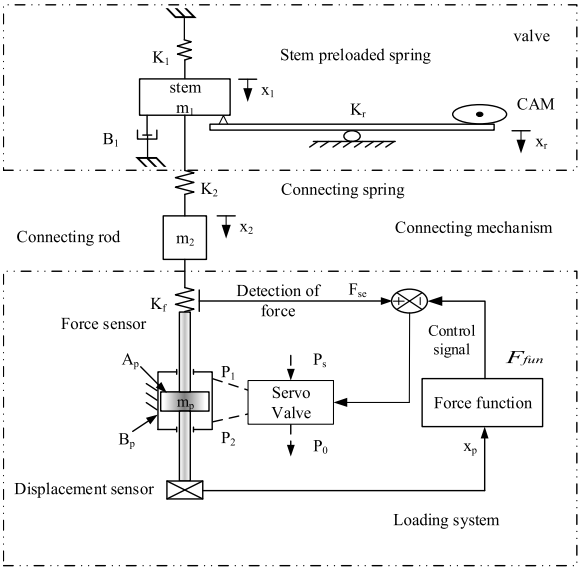

FIGURE 1. Composition diagram of single channel loader system.

As shown in Fig. 1, the steam valve stem moves in a straight line under the action of an external cam drive mechanism (not shown in the composition diagram). The piston rod of

the hydraulic cylinder is connected with the steam valve stem through a connecting member. The function force generator calculates the force acting on the valve stem according to the displacement of the valve stem, and the corresponding loading force is programmed by the force function exerted on the valve stem by the hydraulic cylinder. A force sensor is installed between the piston rod and the valve stem of the hydraulic cylinder to form a force closed-loop control.

Steam stem force loading system adopts symmetrical valve to control the power mechanism of symmetrical cylinder. Before establishing the mathematical model of the system, the following assumptions are made: (1) symmetrical matching of throttle orifice of servo valve; (2) short and thick connection tubes and neglecting the friction losses in pipeline, fluid quality and flow dynamics; (3) laminar leakage at inside and outside hydraulic cylinder; (4) the modulus of elasticity is keep at constant.

A. MATHEMATICAL MODEL OF PASSIVE LOADING SYSTEM

Firstly, according to the characteristics of small displacement, the linear equation of servo valve load flow is obtained near the zero at servo valve.

$$Q_L = K_q x_v - K_c P_L \tag{1}$$

where K_q is the servo valve flow gain, K_c is the valve flow pressure coefficient, x_v is the servo valves pool displacement, P_L is the loading pressure of the servo valve, and Q_L is the loading flow of the servo valve.

The flow continuity equation of the hydraulic cylinder is:

$$Q_L = A_p \dot{x}_p + C_{tc} P_L + \frac{V_t}{4\beta_e} \dot{P}_L \tag{2}$$

where A_p is the piston effective area, x_p is the piston displacement, C_{tc} is the total hydraulic cylinder leakage coefficient, V_t is the total volume of two chambers in hydraulic cylinder, and β_ε is the equivalent elastic modulus.

The influence of friction on the redundant force is indirect, and it indirectly affects the redundant force by influencing the motion state. Besides, the friction force has a certain impact on the tracking accuracy of the loading line, but the influence of the redundant force is much greater than it. So, the nonlinear factors such as coulomb friction and the influence of oil mass are ignored. According to Newton's second law, the force balance equation of mass in Fig. 1 can be written as follows:

$$F_{se} + A_p P_L = m_p \ddot{x}_p + B_p \dot{x}_p \tag{3}$$

$$F_{se} = K_f \left(x_2 - x_p\right) \tag{4}$$

where m_p is the mass of piston assembly, B_p is the Ni hydraulic cylinder viscosity resistance coefficient, F_{se} is the output force of the force transducer or the detection force, K_f is the stiffness of the force transducer, and x_2 is the displacement converted to sensor stem.

At the same time, the force balance equation of mass in Fig. 1 can be obtained as:

$$m_2 \ddot{x}_2 = K_2 \left(x_1 - x_2\right) - F_{se} \tag{5}$$

where m_2 is the quality of connecting parts and valve stem, K_2 is the stiffness of the valve stem and the fittings, and x_1 is the displacement of steam stem. By applying Laplace transform to equations (1) - (5), the block diagram of the hydraulic power mechanism can be drawn shown in Fig. 2.

According to Fig. 2, the transfer function expression that takes stem displacement x_1 and spool displacement x_v as input and force sensor F_{se} as output can be calculated as follows.

$$F_{se} = G_1(s)\, x_v + G_2(s)\, x_1 \tag{6}$$

$$G_1(s) = -\frac{K_q}{K_{ce}} A_p \frac{\frac{m_2}{K_2} s^2 + 1}{A(s)} \tag{7}$$

$$G_2(s) = \frac{A_p^2 s}{K_{ce} K_2} \frac{C(s)}{A(s)} \tag{8}$$

where

$$C(s) = \frac{V_t m_p}{4\beta_e A_p^2} s^2 + \left(\frac{m_p K_{ce}}{A_p^2} + \frac{V_t B_p}{4\beta_e A_p^2}\right) s + \frac{B_p K_{ce}}{A_p^2} + 1$$

$$A(s) = \frac{V_t m_p m_2}{4K_2 K_f K_{ce} \beta_e} s^5 + \left(\frac{m_p m_2}{K_2 K_f} + \frac{V_t m_p m_2}{4K_2 K_f K_{ce} \beta_e}\right) s^4$$

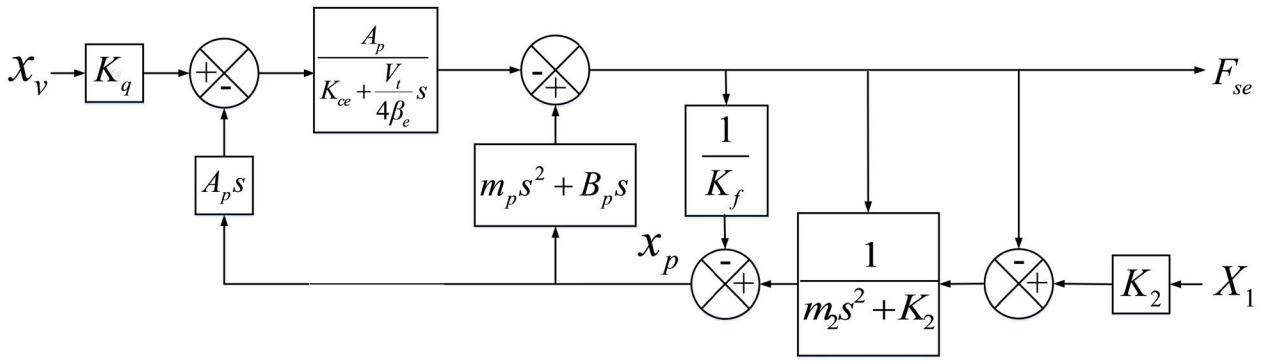

FIGURE 2. Block diagram of the hydraulic servo mechanism.

$$+\left(\frac{m_p m_2}{K_2 K_f}+\frac{V_t m_p}{4K_f K_{ce}\beta_e}+\frac{A_p^2 m_2}{K_f K_{ce} K_2}+\frac{V_t m_2}{4K_2 K_{ce}\beta_e}+\frac{V_t m_p}{4K_2 K_{ce}\beta_e}\right)s^3$$
$$+\left(\frac{m_p+m_2}{K_2}+\frac{V_t B_p}{4K_2 K_{ce}\beta_e}+\frac{m_p}{K_f}+\frac{V_t m_p}{4K_f K_{ce}\beta_e}\right)s^2$$
$$+\left(\frac{A_p^2}{K_2 K_{ce}}+\frac{B_p}{K_2}+\frac{V_t}{4K_{ce}\beta_e}+\frac{B_p}{K_f}+\frac{A_p^2}{K_f K_{ce}}\right)s+1$$
$$K_{\mathrm{ce}}=K_c+C_{tc}$$

where $G_1(s)$ and $G_2(s)$ are the transfer functions of spool displacement, testing force, stem displacement and testing force respectively.

According to Fig. 2, the transfer function expression with displacement of piston rod and servo valve spool as input and force sensor as output can be obtained.

$$F_{se}=\frac{-\frac{K_q A_p}{K_{ce}}x_v+\frac{A_p^2 s}{K_{ce}}C(s)\,x_p}{\frac{V_t}{4K_{ce}\beta_e}s+1} \tag{9}$$

Generally, the bandwidth of the loading system is much smaller than that of the servo valve, so inertia is used to describe the dynamic characteristics of the electro-hydraulic servo valve in the loading system.

$$\frac{x_v}{i_v}=\frac{K_v}{\frac{s}{\omega_v}+1} \tag{10}$$

where i_v is the electro-hydraulic servo valve drive current, ω_v is the servo valve turning frequency, and Kv is the servo valve gain.

In order to establish a complete mathematical model of steam valve stem loading system, the mathematical models of displacement sensor, force sensor, electrical system (signal conditioning, A/D and D/A conversion circuit) and controller are also needed to considered. In engineering, the bandwidth of sensors and electrical systems is larger than that of loading systems, so they can be regarded as proportional links in system modeling. The gain between the voltage signal output of industrial computer through D/A and the driving current of servo valve is K_α, and the units is A/V. The signals detected from displacement sensors and force sensors can be calibrated through the control computer. In order to simplify the problem, this paper deals with it in a one-to-one relationship. The controller model of the loading system is expressed as $G_c(s)$, the redundant force compensation link can be expressed as $G_{cm}(s)$ and $G_{sf}(s)$ is force function. Therefore, the complete block diagram of the loading system can be drawn as shown in Fig. 3.

Equation (9) shows that the sensor detection force F_{se} consists of two parts: the expected force generated by servo valve control and the redundant force generated by cylinder motion. As can be seen from Fig. 2, the redundant force is only related to the speed and acceleration of the loading system. The redundant forces related to the acceleration of the loading system are generated by overcoming the mass inertia force of the piston assembly in the loading cylinder.

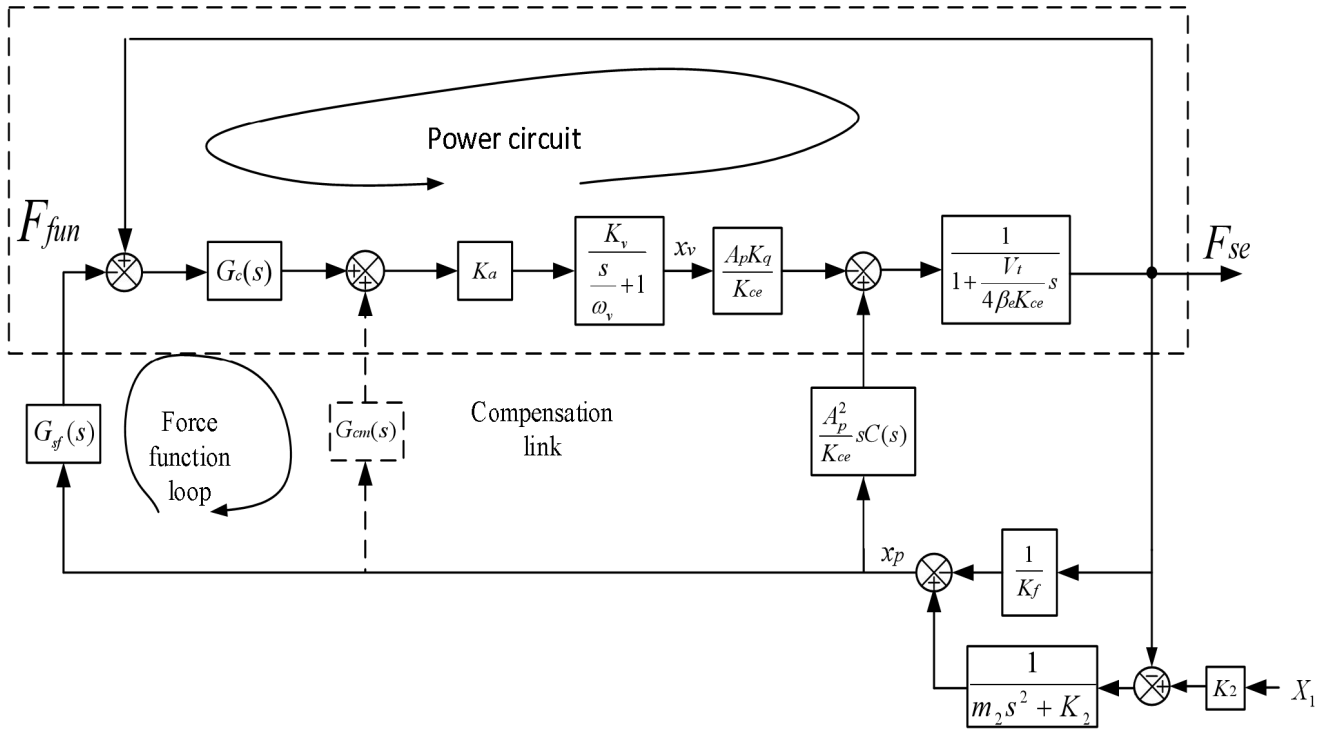

FIGURE 3. Total block diagram of loader system.

The forced flow is the main factor causing the redundant forces.

B. MATHEMATICAL MODEL OF DRIVING FORCE LOADING SYSTEM

When the system works under the active loading condition, the valve stem is fixed. The cam transmission mechanism of the valve stem stops driving, and the driving force loading experiment of the steam valve stem is carried out through the active output of the hydraulic cylinder. In deriving the dynamic mechanism model, the force balance equation is as follow

$$P_L A = m\ddot{x}_p + K_2 x_p \tag{11}$$

where m is the total mass of the system, so the

$$m = m_1 + m_p$$

Referring to equations (1), (2) and (11), the power mechanism block diagram of the driving force loading system can be obtained which is shown in Fig. 4.

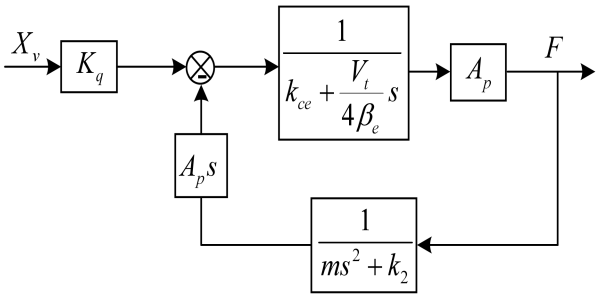

FIGURE 4. Block diagram of static loader system.

According to Fig. 4, the transfer function of the dynamic mechanism in driving force loading system can be expressed as:

$$\frac{F}{X_V} = \frac{\frac{K_q A_p}{K_{ce}}\left(\frac{m}{K_2}s^2+1\right)}{\frac{V_t m}{4\beta_e K_{ce} K_2}s^3 + \frac{m}{K_2}s^2 + \left(\frac{V_t}{4\beta_e K_{ce}} + \frac{A_p^2}{K_2 K_{ce}}\right)s + 1} \tag{12}$$

According to the above expression, a complete model of the driving force loading system can be obtained by referring to Fig. 3 of the force loading system, which is not discussed in detailed. In order to analyze and design the steam valve stem force control system, the physical parameters of the system are given in TABLE 1.

III. STUDY ON CONTROL STRATEGY OF STEAM STEM LOADING SYSTEM

A. DRIVING FORCE CONTROL SYSTEM SIMULATION AND CONTROL STRATEGY

According to the mathematical model of driving force control system and the parameters in TABLE 1, the open-loop frequency characteristics of driving force control system

TABLE 1. The physical values of the force control system.

Parameter	Value
Oil pressure (MPa)	16
Piston rod diameter (mm)	56
The piston diameter (mm)	80
Total stroke of hydraulic cylinder （mm）	110
Elastic modulus of hydraulic oil （MPa）	690
Quality of connecting parts and valve stem （kg）	15
Mass of piston assembly （kg）	35
Stiffness of force transducer (N/m)	1e6
Hydraulic cylinder total leakage coefficient （m^5/Ns）	8.5e-12
Hydraulic cylinder viscous damping coefficient （Ns/m）	10000
Servo valve flow gain （m^2/s）	0.1389
Valve flow pressure coefficient （(m^3/s)/Pa）	4.63e-11
Servo valve gain （m/A）	0.1
Amplifier gain （A/V）	0.01

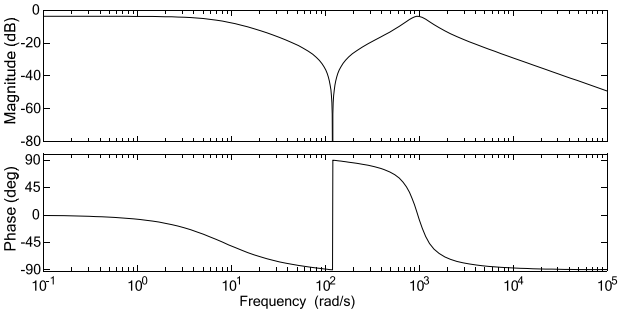

FIGURE 5. Open-loop bode diagram of static loader system.

can be obtained by using the simulation software of MATLAB/Simulink as shown in Fig. 5.

According to the frequency charts, it is necessary to limit the high frequency peak value of the system to ensure the stability margin of the system. In this project, a dual inertia link is added between the first turning frequency and the anti-resonance frequency of the system to limit the high frequency amplitude of the system. The transfer function of the dual inertia link is as follows:

$$G_{ci}(s) = \frac{1}{\left(\frac{s}{\omega_p}+1\right)^2} \tag{13}$$

where ω_p is the double inertia link turning frequency.

The open-loop evaluation characteristics of the driving force control system with dual inertia links are shown in Fig. 6.

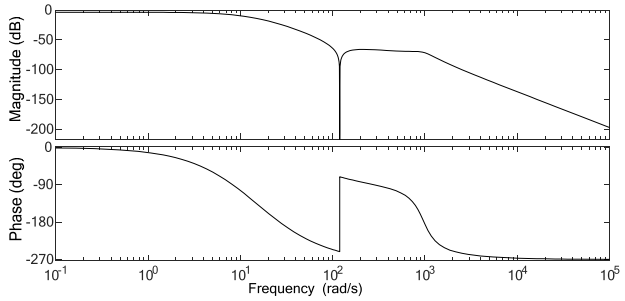

FIGURE 6. Bode diagram of loader system after double inertial loop adjusted.

From Fig. 6, it can be seen that the high frequency amplitude of the system is suppressed. The load stiffness of the loading system has influence on the dynamic characteristics of the system. The stiffness through different load analysis, the open-loop bird diagram of the driving force system is obtained which is shown in Fig. 7.

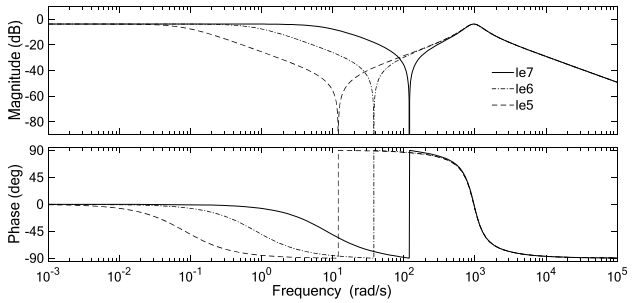

FIGURE 7. Dynamic influence of the load stiffness.

In the driving force control system, the greater the stiffness of the load, the higher the bandwidth frequency of the system.

B. SIMULATION AND CONTROL STRATEGY OF STEM PASSIVE LOADING SYSTEM

Through the above analysis, the redundant force existence affects the control accuracy of loading force. Thus the simple and feasible method of redundant force suppression in engineering is the compensation method based on structural invariance principle. The compensation method based on the structural invariance principle is suitable for compensating low-frequency redundant forces, which is the reason behind the selection of this method in this paper. The invariance principle compensation method is used to compensate the excess force of the piston speed in hydraulic cylinder which is shown in Fig. 3. In Fig. 3, $G_{cm}(s)$ shows the redundant force compensation linkage. This link can be expressed by the following specific expression,

$$G_{cm}(s) = \frac{A_p\left(\frac{s}{\omega_v}+1\right)sC(s)}{K_aK_vK_q} \tag{14}$$

Ideally, the redundant force of the loading system can be completely eliminated by using equation (14) in order to compensate the redundant force, so that the transfer function of the compensated power mechanism can be the first-order inertia link, and the loading system cannot be affected by the change of load. There are higher order differential components in the compensation link, so it is difficult to realize the complete compensation of surplus force. In addition, due to the influence of model error, nonlinearity and varying time parameters, it is difficult to completely compensate the redundant force and the system will be affected by the load. In steam stem loading system, the low frequency part redundant force is compensated which can meet the indexed requirements. Therefore, in order to simulate mass force and damping force, the compensation link includes the velocity and acceleration terms. Neglecting the influence of acceleration and servo valves terms, the compensation link expression under partial compensation can be obtained as follows:

$$G_{cm}(s) = \left(\frac{V_tB_p}{4\beta_eA_pK_aK_vK_q} + \frac{K_{ce}m_p}{A_pK_aK_vK_q}\right)s^2 + \left(\frac{A_p}{K_aK_vK_q} + \frac{K_{ce}B_p}{A_pK_aK_vK_q}\right)s \tag{15}$$

According to the above mathematical model, the valve stem displacement is used as the input to the system's redundant force simulation. The displacement signal of valve stem is $y = 0.045\sin(2\pi \times 0.1t)$, and the connection stiffness is K_2 whose value is respectively le5, le6 and le7. The simulation results are shown in Fig. 8.

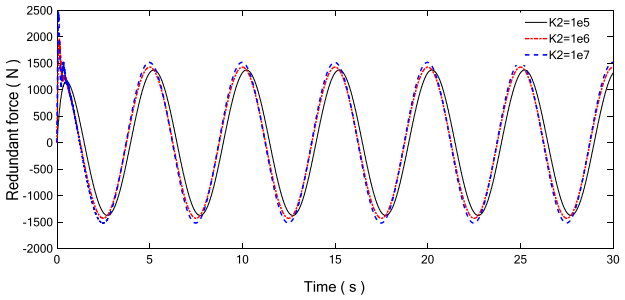

FIGURE 8. Simulation result of redundant force.

As can be seen from Fig. 8, the size of the joint stiffness has a great influence on the magnitude of the redundant force, and the greater the connecting stiffness, the greater the redundant force. However, redundant force does not create much difference. Moreover, in order to consider the dynamic performance of active loading, the loading system connection stiffness range is selected from le5 to le6. Equation (15) is used to suppress the redundant force as the result is shown in Fig. 9.

The simulation results show that after the partial compensation of structural invariance principle, the surplus torque of the system is controlled within 3%. However, the compensation effect of the principle of structural invariance is poor when the valve rod starts and stops. At this time, reducing

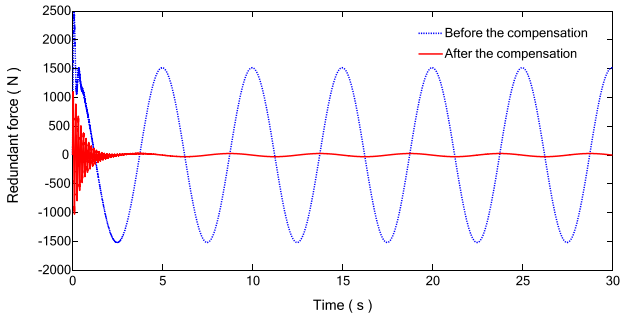

FIGURE 9. Results of redundant force compensation.

the connection stiffness is necessary to further reduce the redundant force (the bandwidth of the servo valve is certain).

Combined with the schematic diagram of the loading system in Fig. 3, the valve stem loading system is simulated by using the principle of structural invariance and double inertia links, and the results are shown in Fig. 10.

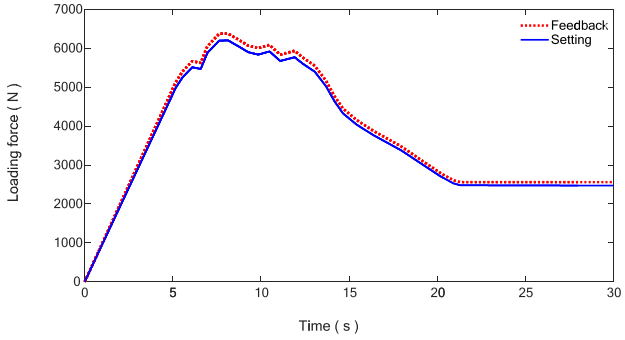

FIGURE 10. Diagram of simulation results of loading system.

The set force signal in Fig. 10, namely the force function shown in Fig. 3, is the data obtained through experiments, and then the force loading signal is obtained by looking up the table in Matlab/Simulink. It can be seen from Fig. 10 and Fig. 11 that the whole loading system has a high control accuracy and the error signal is also within the tolerance range.

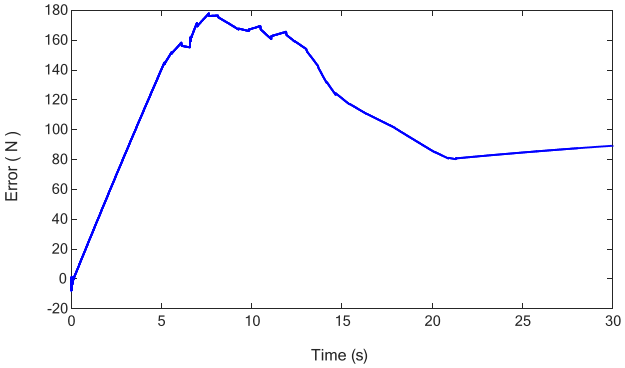

FIGURE 11. Loading system error signal (Tolerance 300N).

IV. DESIGN OF CONNECTION COMPONENT FOR STEAM STEM LOADING SYSTEM

One end of the steam stem loading assembly is connected with the hydraulic cylinder and the other end is connected with the driving system, which is used to transfer the plunger movement output of the hydraulic cylinder to the driving system, and plays a key role of fixing and supporting. Furthermore, there are force sensors inside the loading component, which can transform the system force into the electrical signals and transmit them to the control system. In above simulation studies, it can be seen that the connecting component stiffness directly affects the magnitude of the redundant force. Therefore, it is very important to design the appropriate stiffness connecting component for the loading system. The structure of the stem loading assembly is shown in Fig. 12.

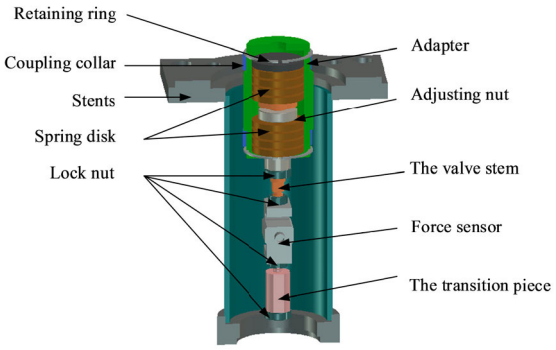

FIGURE 12. Structural diagram of stem loading connection components.

As can be seen from the Fig. 12, the stiffness of the stem loading connection component is adjusted by two sets of butterfly springs in parallel. At this point, the stiffness calculation diagram of the connecting component is shown in Fig. 13.

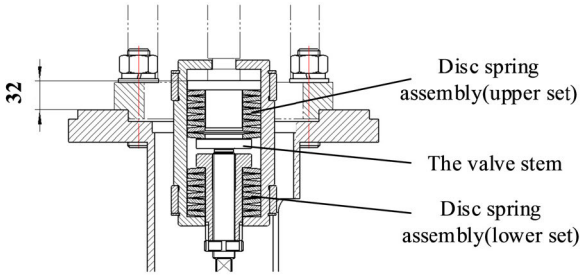

FIGURE 13. Schematic diagram of stiffness calculation of connecting components.

As shown in Fig. 13, the one-ton valve elastic device consists of two groups of disc spring components, each group of disc spring components is composed of 8 disc springs of type Φ80/Φ41A, one group is arranged on both sides of the valve stem. The bearing capacity equation of a single disc spring of Φ80/ Φ41A type is as follows:

$$F = \frac{4Et^4}{K_1 D^2(1-m^2)} K_4^2 \frac{f}{t}\left[K_4^2\left(\frac{h_0}{t}-\frac{f}{t}\right)\left(\frac{h_0}{t}-\frac{f}{2t}\right)+1\right] \quad (16)$$

where E is the modulus of elasticity, which is 2.061×10^5 MPa, μ is Poisson's ratio which is 0.3, D means the outer diameter of the spring is 80mm, t means the spring thickness is 5 mm, h_0 is the deformation under pressure of the spring with a size of 1.7mm, f is the amount of spring deformation, K_1 and K_4 are calculated coefficients, which are 0.83 and 1 respectively.

At the initial pretightening, the initial pre-compression quantity is 3.2mm, and the preloading force is 1.38×10^4 N. When the hydraulic cylinder works and the total deformation of the elastic device, f is 1.6 mm, the upper disc spring component is extended by 1.6mm and the lower disc spring component is compressed by 1.6 mm. Therefore, the total deformation of the upper disc spring component is 1.6 mm, and the deformation of a single disc spring is $f_1 = 0.2$ mm. The total deformation of the lower disc spring component is 4.8 mm, and the deformation of a single disc spring is $f_2 = 0.6$ mm. At this time, the bearing capacity of the upper disc spring component is $F_1 = 5.65 \times 10^3$ N. The bearing capacity of the following disc spring component is $F_2 = 1.64 \times 10^4$ N, the output of the hydraulic cylinder is $F = F_1 + F_2 = 1.07 \times 10^4$ N, and the stiffness of the entire elastic device is $k = F/f = 6.69 \times 10^6$ N/m. The simulation conclusion above is satisfied.

V. EXPERIMENTAL STUDY ON STEAM STEM LOADING SYSTEM

Steam stem loading system adopts xPC-based rapid prototype control technology, which keeps the hardware architecture of upper and lower computer. The system composition is shown in Fig. 14.

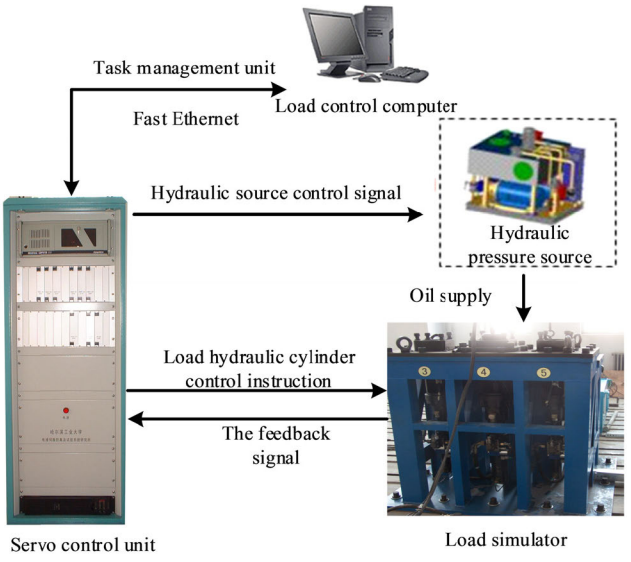

FIGURE 14. Structural diagram of loading system composition.

As shown in Fig. 14, the loading control computer is the task management unit, which is responsible for the human-computer interaction of loading system experiment monitoring, data storage and display. The lower computer realizes the real-time control of loading system, which is the core of servo control unit. The data acquisition card is configured to realize the collection of field sensor signals and servo valve driving signals. The upper computer uses Labview to compile the monitoring interface, and the lower computer uses MATLAB/Simulink to compile the real-time control software. The hydraulic source in Fig. 15 provides power for the loading system, converts hydraulic energy into mechanical energy, and realizes the simulation of the mechanical environment of the valve stem. Active and passive loading experiments were carried out with the loading system. The operating interface of the loading system is shown in Fig. 15.

FIGURE 15. Upper computer interface of loading system.

As shown in Fig. 15, the upper computer interface of the loading system is mainly divided into display and operation parts, which mainly display experimental curves, system faults and alarms, etc. The operation part includes the selection of control channel, power station control, data storage and signal generator functions. Active and passive loading experiments are carried out on the valve stem.

The experimental results are shown in Fig. 16 and Fig. 17 respectively. From Fig. 16, it can be seen that the overshoot of the loading system is controlled within 5%, the rise time is within 0.1s, and the static error of the system is controlled within 3% to meet the requirements of accuracy and speed in the loading test. It can be obtained from Fig. 17 that the load tolerance of the loading system can be controlled within 300N

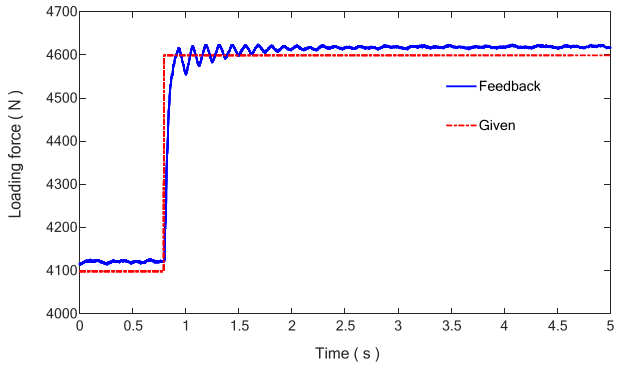

FIGURE 16. Curve of step response under active loading.

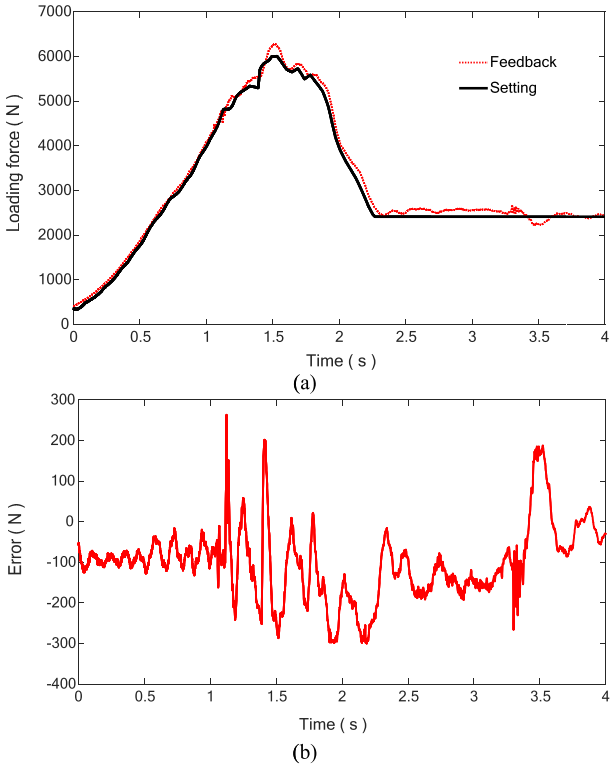

FIGURE 17. (a) Tracking curve of passive experiment. (b) Error curve of passive experiments.

under the condition that the partial invariance structure principle is adopted, which meets the accuracy requirements of the valve stem loading system.

The real time control program of lower computer is shown in Fig. 18. Protection logic module is mainly used for system protection. The pump control module is mainly used for the start and stop of the pump. The data acquisition module is mainly used for force, displacement, speed signal acquisition, servo valve drive (A/D) signal acquisition and digital I/O (D/A) acquisition. The system closed loop is mainly used for the control of displacement, driving force and passive loading. The fault detection module is mainly used for force and displacement over-limit detection. Communication module is mainly used for data upload to the upper computer and data display and storage.

VI. CONCLUSION

Since the system has light mass, large stiffness and high hydraulic natural frequency, the bandwidth of servo valve determines the bandwidth of active loading, which further affects the tracking accuracy. On the other hand, the bandwidth of servo valve has a great influence on the compensation effect of redundant force. The faster the response of servo valve is, the better the compensation effect is.

The connection stiffness of the loading system is the series stiffness of the force sensor and the connecting spring. From the simulation results, it can be found that the connection stiffness has an influence on the redundant force. The smaller the stiffness is, the smaller the redundant force is. When the structure invariant principle is applied to compensate the redundant force, the redundant force can be almost eliminated in the steady state (when the stem moves uniformly). However, when the valve stem starts and stops, the compensation effect based on the principle of structure invariance is

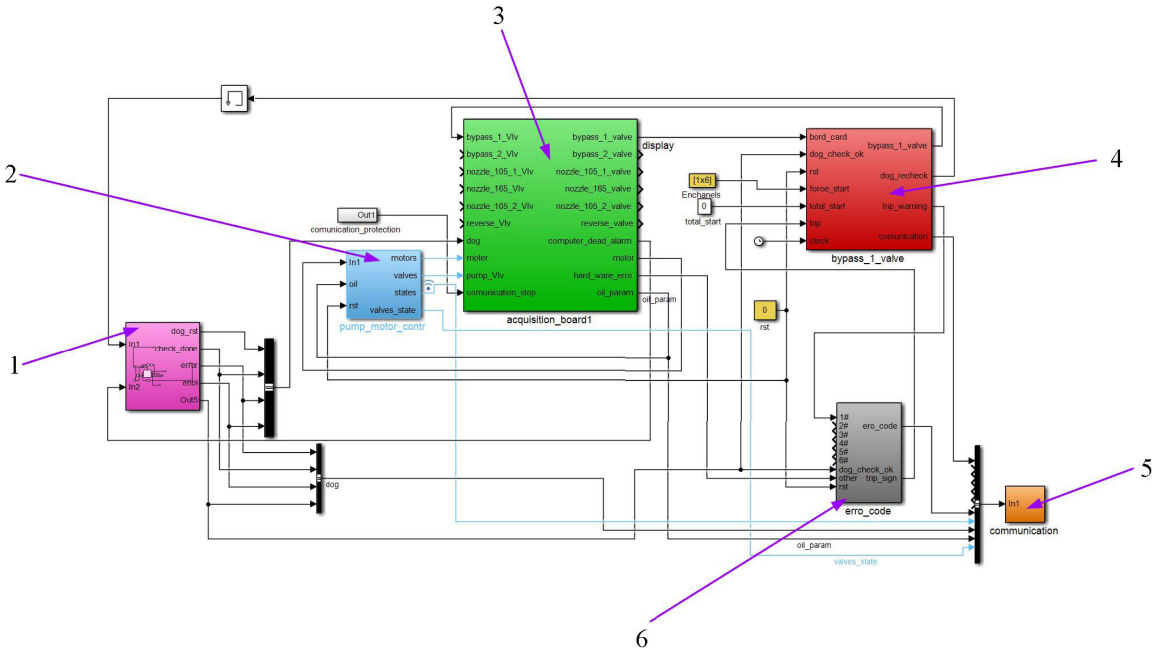

FIGURE 18. Real-time control program of lower computer. 1. Protection logic module; 2. Pump control module; 3. Data acquisition module; 4. Closed loop system; 5. Fault detection module;6. Communication module.

unsatisfactory. At this time, we can further reduce the redundant force by reducing the connection stiffness and effective area (the bandwidth of servo valve is fixed). The stiffness of the connection assembly designed in this paper is 6.96e6, which can take into account both active and passive loading.

Based on the rapid prototyping control method, it is verified that the partial structure invariance compensation method can effectively suppress the redundant force of passive loading and meet the requirement of tolerance to 300N. It is also verified that the dual inertia link is effective to control the active and passive loading systems.

REFERENCES

[1] K. Chen, S. Y. Xu, and Y. D. Zhang, "Design and check of spring for steam turbine admission valve actuator," *J. Dongfang Turbine*, vol. 3, pp. 10–15, Sep. 2017.
[2] J. S. Zhao, Z. M. Ye, G. Shen, and J. W. Han, "Redundant force restraining for the control loading system of a flight simulator," *J. Harbin Eng. Univ.*, vol. 33, no. 8, pp. 1008–1015, 2012.
[3] C. Xiao, X. H. Jin, M. W. Zhang, and B. J. Zhen, "Research on superfluous force of passive electro-hydraulic loading system," *J. Machinery Des. Manuf.*, vol. 9, pp. 71–75, Sep. 2018.
[4] M. Zhao and Z. M. Fan, "A method of high-frequency redundant-torque suppression for nonlinear time-varying loading systems," *J. Electron. Des. Eng.*, vol. 26, no. 23, pp. 134–138, 2018.
[5] G. Q. Li, W. Liu, and W. F. Han, "Research on synchronous structure decoupling of electro-hydraulic load simulators," *J. China Mech. Eng.*, vol. 28, no. 24, pp. 2931–2939, 2017.
[6] J. Wang, "Study on eliminating the superfluous force of marine electrohydraulic load simulator applied with dual-valve parallel connected control," *J. Mech. Eng.*, vol. 41, no. 4, p. 229, 2005.
[7] P. G. Qi, Q. T. Huang, and H. Z. Jiang, "Hydraulic control loading system based on position control," *J. Jilin Univ. (Eng. Technol. Ed.)*, vol. 38, no. S2, pp. 128–133, 2008.
[8] J. Zhao, G. Shen, C. Yang, W. Zhu, and J. Yao, "A robust force feedforward observer for an electro-hydraulic control loading system in flight simulators," *ISA Trans.*, vol. 89, pp. 198–217, Jun. 2019.
[9] J. Zhao, Z. Wang, C. Zhang, C. Yang, W. Bai, and Z. Zhao, "Modal space three-state feedback control for electro-hydraulic servo plane redundant driving mechanism with eccentric load decoupling," *ISA Trans.*, vol. 77, pp. 201–221, Jun. 2018.
[10] M. Khamar and M. Edrisi, "Designing a backstepping sliding mode controller for an assistant human knee exoskeleton based on nonlinear disturbance observer," *Mechatronics*, vol. 54, pp. 121–132, Oct. 2018.
[11] Z.-C. Zhu, X. Li, G. Shen, and W.-D. Zhu, "Wire rope tension control of hoisting systems using a robust nonlinear adaptive backstepping control scheme," *ISA Trans.*, vol. 72, pp. 256–272, Jan. 2018.
[12] G. Yang and J. Yao, "Output feedback control of electro-hydraulic servo actuators with matched and mismatched disturbances rejection," *J. Franklin Inst.*, vol. 356, no. 16, pp. 9152–9179, Nov. 2019.
[13] H.-B. Yuan, H.-C. Na, and Y.-B. Kim, "Robust MPC–PIC force control for an electro-hydraulic servo system with pure compressive elastic load," *Control Eng. Pract.*, vol. 79, pp. 170–184, Oct. 2018.
[14] W. Gu, J. Yao, Z. Yao, and J. Zheng, "Output feedback model predictive control of hydraulic systems with disturbances compensation," *ISA Trans.*, vol. 88, pp. 216–224, May 2019.
[15] W. Han, L. Xiong, and Z. Yu, "Braking pressure control in electro-hydraulic brake system based on pressure estimation with nonlinearities and uncertainties," *Mech. Syst. Signal Process.*, vol. 131, pp. 703–727, Sep. 2019.
[16] X. Yin, W. Zhang, Z. Jiang, and L. Pan, "Adaptive robust integral sliding mode pitch angle control of an electro-hydraulic servo pitch system for wind turbine," *Mech. Syst. Signal Process.*, vol. 133, Nov. 2019, Art. no. 105704, doi: 10.1016/j.ymssp.2018.09.026.
[17] Y. Sang, W. Sun, F. Duan, and J. Zhao, "Bidirectional synchronization control for an electrohydraulic servo loading system," *Mechatronics*, vol. 62, Oct. 2019, Art. no. 102254, doi: 10.1016/j.mechatronics.2019.102254.
[18] K. Guo, J. Wei, J. Fang, R. Feng, and X. Wang, "Position tracking control of electro-hydraulic single-rod actuator based on an extended disturbance observer," *Mechatronics*, vol. 27, pp. 47–56, Apr. 2015.
[19] Q. Guo, J.-M. Yin, T. Yu, and D. Jiang, "Coupled-disturbance-observer-based position tracking control for a cascade electro-hydraulic system," *ISA Trans.*, vol. 68, pp. 367–380, May 2017.
[20] C. Jing, H. Xu, and J. Jiang, "Dynamic surface disturbance rejection control for electro-hydraulic load simulator," *Mech. Syst. Signal Process.*, vol. 134, Dec. 2019, Art. no. 106293, doi: 10.1016/j.ymssp.2019.106293.
[21] C. Liu, G. Luo, Z. Chen, W. Tu, and C. Qiu, "A linear ADRC-based robust high-dynamic double-loop servo system for aircraft electro-mechanical actuators," *Chin. J. Aeronaut.*, vol. 32, no. 9, pp. 2174–2187, Sep. 2019.
[22] G. Shen, Z.-C. Zhu, X. Li, Y. Tang, D.-D. Hou, and W.-X. Teng, "Real-time electro-hydraulic hybrid system for structural testing subjected to vibration and force loading," *Mechatronics*, vol. 33, pp. 49–70, Feb. 2016.
[23] C. Wang, Z. Jiao, S. Wu, and Y. Shang, "Nonlinear adaptive torque control of electro-hydraulic load system with external active motion disturbance," *Mechatronics*, vol. 24, no. 1, pp. 32–40, Feb. 2014.

BING ZHANG received the Ph.D. degree from the Harbin Institute of Technology, China, in 2013. He currently works with Jiangsu University. His main research interests include electro-hydraulic servo control systems, vibration control technology, embedded control technology, and parallel robot.

HUA HUANG is currently pursuing the master's degree in mechanical engineering with Jiangsu University, Zhenjiang, China. His main research interest includes electro-hydraulic servo control systems.

JIAMIN CAI is currently pursuing the master's degree in mechanical engineering with Jiangsu University, Zhenjiang, China. His main research interest includes vibration control technology.

ZILIANG JIANG is currently pursuing the master's degree in mechanical engineering with Jiangsu University, Zhenjiang, China. His main research interests include electro-hydraulic servo control systems and robot design and control.

PENGFEI QIAN received the Ph.D. degree from Zhejiang University, China, in 2014. He is currently an Associate Professor with the School of Mechanical Engineering, Jiangsu University. His main research interests include fluid power transmission and control technology, development and control of novel pneumatic components, and application of nonlinear control theory.